11TH INTERNATIONAL SYMPOSIUM ON PARTICLE IMAGE VELOCIMETRY – PIV15
Santa Barbara, California, September 14-16, 2015

Near-wall turbulence characterization using 4D-PTV Shake-The-Box

Andreas Schröder[1], Daniel Schanz[1], Reinhard Geisler[1], Sebastian Gesemann[1] and Christian Willert[2]

[1] Institute of Aerodynamics and Flow Technology, DLR, Göttingen, Germany
[2] Institute for Propulsion Technology, DLR, Cologne, Germany
andreas.schroeder@dlr.de

ABSTRACT

A near-wall flow characterization including measurements of instantaneous wall-shear stresses of a turbulent boundary layer (TBL) developing along a flat plate with zero pressure gradients has been performed by using two advanced particle based measurement methods. The experiments were conducted in the 1m- wind tunnel facility of Göttingen at U_∞ = 10 m/s and a Reynolds number of Re_θ = 2,770 corresponding to Re_τ = 960. First, high-speed 2C-PIV was performed at two image magnification factors at 2 kHz and 4 kHz frame rates in order to obtain the overall statistical properties of the boundary layer profile together with a large time series of instantaneous 2C velocity vector fields in a streamwise, wall-normal plane. Single pixel line correlation applied to the particle image area close to the wall provided high spatial resolution velocity data down into the viscous sublayer. In a second step, the novel 4D-PTV technique Shake-The-Box (STB) was applied to a time series of particle images acquired with a typical tomographic high-speed camera set-up at 15.873 kHz. The STB measurement domain consists of a wall-bounded volume covering a stream- and spanwise area of 430 x 430 viscous units ($l^+ = \nu/u_\tau$) and a wall-normal extension of 32 viscous units. A comprehensive set of relatively dense Lagrangian track data was reconstructed from two time resolved sequences of 115,000 time steps each. The data enables an accurate and very high resolution measurement of the mean and rms-velocity profiles averaged in bins sized by a fraction of a viscous unit, of both components of the instantaneous wall shear stress (τ^+_w) and all components of the Reynolds stress tensor. Furthermore, the time-resolved 3D velocity vectors and corresponding gradient tensor have been interpolated onto a regular grid using the time series of irregularly distributed Lagrangian track data. With the present data coherent structures and their dynamics close to the wall can be investigated together with their role for various (rare) wall shear stress events. The STB method is proven capable of coping with strong velocity gradients close to walls and can also be extended to TBL flows with much higher Reynolds numbers.

INTRODUCTION

The role of turbulent flow features for the momentum transport near walls and corresponding (large) wall-shear stress events are prominent research topics for aerodynamics and technical flows. Large portions of the total aerodynamic drag are produced by skin friction along surfaces underneath turbulent boundary layers (TBL). Therefore, a better understanding of the related fluid dynamics is of high importance for advanced drag reduction strategies, high-lift-configuration design and the enhancement of flow- and separation control devices. Furthermore, advanced CFD validation procedures and recent LES wall-model developments requires accurate (and time-resolved) near-wall turbulence data at high Reynolds numbers provided by statistically converged data-sets. Nowadays, DNS of TBL flows is limited to moderate Reynolds numbers (Re_θ < 5,000), so that appropriate measurement techniques that are able to deliver unsteady (or even time-resolved) three-component velocity information at industrially relevant Reynolds numbers at high spatial and temporal resolution, preferably at many points simultaneously, are highly welcome. All known measurement techniques are confronted with significant challenges in providing reliable data in close proximity to rigid surfaces due to strong mean and instantaneous velocity gradients. The use of accurate probe measurement techniques is limited due to its intrusiveness, coupling effects with the wall and spatial extensions (causing low-pass filtering effects) [1] and even modern miniaturized (pulsed) hot-wire probes or µLDA systems [2][3] are still suffering from spatial filtering effects close to the wall and are only capable of providing single-point information. So far on the experimental side only oil-film interferometry [4][5] is a widely accepted method for delivering the mean wall-shear stress magnitude and skin friction coefficient C_f value accurately. Nevertheless, in order to understand the (near-wall) boundary layer flow causing specific wall-shear stress events and producing drag a pure measurement of C_f would need to be complemented. In this sense a method is desired that is capable of providing both

both components of the unsteady wall-shear stress along with the friction velocity vector and at the same time provides multi-point 3C-velocity vectors in the near wall region in a non-intrusive manner, without biasing effects and at high accuracies. Therefore we will first have a look on recent developments of non-intrusive particle based planar and volumetric measurement methods.

PIV has undergone significant progress in the past three decades in terms of spatial and temporal resolution [6]. Within the recent years tomographic PIV [7] has matured into a reliable tool for investigating turbulent flows and delivering the complete 3D velocity gradient tensor [8]. However for all PIV based approaches the spatial resolution of the local instantaneous velocity measurement is limited by the finite size of the cross-correlation window, which acts as a low-pass filter biasing the measurement particularly in presence of strong velocity gradients. Two further basic limitations of PIV can be described by the dynamic velocity range (DVR) which is typically in the order of 1:100 and the dynamic spatial range (DSR), which is basically limited by the resolution of the employed camera sensor [9]. Several methods have been developed in order to overcome these limitations; nevertheless, only particle-tracking approaches have been found capable of delivering reliable results for at least the mean flow statistics near interfaces and walls [10] or in strong-shear flow. The first successful experiment using a 3D particle tracking method in the near wall region of a moderate Reynolds number turbulent channel flow at Re_τ = 1,400 was based on digital holographic particle microscopy: A reconstruction of 3D particle distributions of a series of frame-straddled double images has been realized by Sheng et al. [11]. Results of mean and rms-profiles, fluctuation components of the wall-shear stress and spatial topologies of some velocity vector volumes in the direct vicinity of the wall have been presented. Nevertheless, the temporal resolution, a higher accuracy of the velocity estimation and statistical convergence for higher order moments are still missing.

Recently, the Shake-The-Box (STB) technique [12][13] has been developed, which is a 4D-PTV evaluation method for densely seeded flows capable of coping with ill-posed 3D particle reconstruction problems based on few camera projections by seizing the temporal information with predictive steps and applying an iterative particle reconstruction and image matching scheme (see Iterative Particle Reconstruction [14]). Within the resulting dense Lagrangian tracks the STB technique uses temporal fitting functions based on optimal Wiener filtering along all found particle paths. The parameters of an optimal Wiener filter are determined from statistical properties of the Lagrangian position, velocity and acceleration fluctuations along the reconstructed 3D particle positions and tracks for all three components separately. This optimal temporal filtering approach enables an accurate estimation of position, velocity and acceleration vectors and enhancing the DVR to values > 1:1000, when sufficient track lengths are provided. Therefore, STB is able to deliver accurate mean- and Reynolds stress values by bin-averaging (down to sub-pixel spatial resolution) and additionally provide the complete instantaneous velocity gradient tensor at a relatively high spatial resolution (comparable to a very well resolved tomographic PIV measurement) by using a proper interpolation scheme given with the “Flow-Fit” algorithm that was recently developed by DLR (brief description in [15]). Therefore it is expected that with STB valuable data for turbulence characterization with outstanding temporal and spatial resolution especially in (wall bounded) shear flow can be obtained.

In general, there is a strong need in fluid mechanics and turbulence research for defining scaling parameters which enable the description of mean and unsteady characteristics of turbulent flows in the form of laws, (self-similar) statistics and trends based on respective definitions of Reynolds numbers. In turbulent boundary layer (TBL) flows with zero pressure gradients (ZPG) mainly two scaling variants are used: The so called “outer scaling” is based on the boundary layer thickness δ, while the “inner scaling” is based on the friction velocity:

$$u_\tau = \sqrt{\frac{\tau_w}{\rho}} = \sqrt{\nu \frac{\partial u}{\partial y}|_{y=0}} \; .$$

Here τ_w is the mean wall-shear stress, ρ the density and ν the kinematic viscosity of the fluid. With the friction velocity u_τ a direct normalization of all measured velocities and length units can be realized. By the definition of a viscous length unit $l^+ = \nu/u_\tau$ the wall-normal position for instance is converted to a non-dimensional unit $y^+ = y/l^+$ (s.c. wall unit). Consequently, for all normalized parameters and statistics based on inner scaling an accurate estimation of the wall-shear stress and wall-position is mandatory. The mean wall-shear stress can be estimated by the velocity gradient within the viscous sub-layer $y^+ < 5$ in which a linear velocity profile can be assumed down to the wall. While accepted throughout the community, it should be noted that this scaling in principle only applies to the mean quantities. In practice however, the TBL unsteady flow may be nonlinear in the immediate proximity of the wall ($y^+ < 4$) due to high speed bursts or other extreme events, which is indicated as well by the present STB data. As pointed out by Brücker [16] the classical definition of the $y^+ = 5$ thickness of the viscous sublayer may need some revision in the context of unsteady near wall fluid dynamics of the TBL.

Today, there is still a need for improved measurement methods that can deliver the distribution of (instantaneous) wall shear-stresses and related skin-friction coefficients C_f together with near-wall velocity field information, especially at high Reynolds numbers. Furthermore, there is a strong necessity of accurately estimating the wall position [17] in order to calculate the wall normal velocity gradient *du/dy* correctly and perform accurate statistics for all profiles normalized by the

corresponding friction velocity u_τ. When using probe measurement techniques there are intrinsic difficulties and uncertainties of applying proper (optical) measurement techniques to achieve the relative probe position. Even with accurate position information the measured mean velocity profile and respective fluctuation component are still biased close to the wall due to intrusiveness and spatial filtering effects. A way to correct for biased probe measurement results applies assumptions of the linear profile or the self-similarity of the *u*-velocity PDF close to the wall [1]. Nevertheless, a direct non-intrusive and statistically bias-free measurement of all three velocity components near the wall and the wall-position itself would be preferable, especially because at high and aerodynamically relevant Reynolds numbers probe techniques reach ultimately their hardware limits. Based on results from DNS and a set of measurement data a formula has been built estimating the Reynolds number trend of the normalized RMS-value of the wall-shear stress to $\tau^+_{w,\,rms} = 0.298 + 0.018 \cdot \ln(\mathrm{Re}_\tau)$ [18]. The low-pass filtering effect of a limited hot-wire length of $l > 11 \cdot l^+$ produces a parallel shifted line at $\tau^+_{w,\,rms} = 0.240 + 0.018 \cdot \ln(Re_\tau)$ [19] for a series of high Reynolds number measurements. The authors correct for this effect by using low Reynolds number DNS values of the universal high-frequency part of the $\tau^+_{w,\,rms}$ distribution.
In recent DNS it has been observes that for increasing Reynolds numbers a growing fraction of the wall-shear stress is negative [20][21], which implies reverse flow events close to the wall, while Eckelmann wrote 1974 based on experimental investigations at relatively low Reynolds number turbulent channel flows using hot-wire and hot-film techniques [22]: “It can be stated with certainty, therefore, that there are no negative velocities near the wall”.

Planar sensor array techniques which are mounted close to or at the wall surface like micro-pillars [23] or film-based methods [24] are delivering both components of the instantaneous friction velocities u_τ and w_τ with only slight intrusive interaction (micro-pillars cross through the viscous sublayer and surface films moves slightly), but need to be calibrated carefully, have a limited accuracy and show frequency response filtering properties. Both techniques would need a combination and synchronization with velocity measurement techniques in the flow region above the wall in order to gain insight into the near-wall flow dynamics and its effect on the measured wall-shear stresses.

For PIV methods the only way of resolving larger parts of the huge range of scales involved in high Reynolds number TBL flows is combining several cameras simultaneously in order to create large fields-of-view where low-frequency events dominate and additionally embed (µ)PIV resp. PTV systems with a large image magnification in order to view details of small scale flow structures and strong velocity gradients e.g. in a region close to the wall enabling the measurement of the mean [25] and instantaneous wall shear stress (slightly low-pass filtered) [26].

The above mentioned and other numerous efforts in developing and applying probe and particle based optical measurement methods in high Reynolds number turbulent shear flow are getting closer and closer to the desired goal, but they are (more or less) complementary and still limited at required resolutions either spatially, temporally or both. In the present work STB shall be introduced as a measurement method which offers the capabilities of delivering 3D non-intrusive, bias-free and high spatially and temporally resolved velocity (and acceleration) data for turbulent shear flow investigations. On the hardware side STB requires a typical multi-camera tomographic particle imaging system *and* time-resolution of the particle illumination and imaging with respect to the flow motion. So far appropriate time-resolved tomographic PIV experiments, which served as data for STB evaluations, have only been realized in low-speed water flows [12][15]. One way to overcome the hardware limitations in order to achieve particle tracking in high speed flows is the proposed multi-pulse STB approach (Novara et al. [27]). The other possibility is pushing the limits of existing hardware. Usually in relevant low-speed air flows (typically $U_\infty > 5$ m/s) the time-resolution of 3D PIV measurements using aerosol particles sized at $d_p \sim 1$µm is limited to the frame-straddling method due to camera frame rate- and laser power limitations. In order to reach particle image frame rates of $f > 15$ kHz useful for particle tracking over many time-steps in low-speed air flows the resolution of existing cameras has to be reduced together with the size of the illuminated measurement volume. Today, high-speed CMOS cameras are available which deliver up to 25 kHz frame rates at 1 Mpx resolution (unfortunately often with relatively large pixel sizes). Together with pulse-burst lasers [28][29], which are capable of emitting pulse trains in the order of typically 10 to 100 laser pulses at very high frequencies (up to the MHz regime) and at laser pulse energies in the order of 5 to 200 mJ such cameras aligned in a tomographic set-up would enlarge the capabilities of STB for densely seeded Lagrangian turbulence investigations in a large variety of subsonic flows: small tracer particles in relatively large volumes could be illuminated sufficiently at several successive time steps enabling convergence of the STB algorithm even for high seeding densities [13], while pixel locking effects due to large pixel sizes of present high-speed cameras could be diminished using diffusor disks in front of the camera lenses.

Compared to such high cost solutions an efficient high-repetition 2C-PIV application for calculating turbulence statistics of a low Reynolds number turbulent boundary layer flow in air has been developed and performed by Willert [30] and will be applied in the following to characterize the overall boundary layer. In the second part of this paper the STB technique will be employed to provide, unsteady time-resolved 3-D data in the near-wall region.

EXPERIMENTAL SET-UP AND PROCEDURE

In the present study a high-repetition 2C-PIV implementation as described in [30] was applied at two large image magnification factors to characterize the turbulent boundary layer flow at U_∞ = 10 m/s free stream velocity covering the boundary layer flow over its whole thickness δ in *y*-direction in order to gain the overall statistical properties. Furthermore, STB has been applied to a thin wall-parallel volume at a high framing rate of 15.873 kHz in order to characterize near-wall turbulence and its spatial and temporal structures at a significant Reynolds numbers in air flow at very high spatial resolution. The measurement campaign was performed in the closed test section of the newly refurbished 1m-Wind Tunnel at DLR Göttingen with a cross-section of 740 x 1,000 mm^2 and a test section length of 3,000 mm. The boundary layer has been tripped by sandpaper stripes and zig-zag bands right after the contraction section. For both experiments DEHS particles with a mean diameter of ~ 1µm were generated by Laskin nozzles and introduced into the circuit wind tunnel enabling a homogenous distribution with adaptable seeding densities within the measurement volumes. The coordinate *x* refers to the streamwise direction while *y* and *z* respectively represent the wall-normal and spanwise directions. At a free stream velocity of U_∞ = 10 m/s the tripped boundary layer flow develops along *x* = 2 m at the lower wall of the test section to a zero pressure gradient turbulent boundary layer (TBL) (see Figure 1) with a Reynolds number based on the momentum thickness of Re_θ = 2,770 corresponding to Re_τ = 960, based on the friction velocity and boundary layer thickness δ_{99}. At the chosen stream-wise position the boundary layer thickness is estimated by the high-resolution profile 2C-PIV method at δ = 43.2 mm and δ_{99} = 35.4 mm with a skin friction velocity of u_τ = 0.418 m/s and corresponding wall-unit size of l^+ ~ 36.58 µm (see Table 2 for further quantities). Then the viscous sub-layer height of y^+ = 5 corresponds to *y* = 183 µm. For the estimation of general measures two sets of in total ~100,000 particle images have been used for the statistics based on two large magnification and high-repetition 2C-PIV profile measurements.

For the corresponding set-up a roughly 5 mm wide measurement area was illuminated by a pair of relatively small sized externally modulated continuous wave lasers (*Kvant Laser*, Slovakia) with a combined output power of about 10 W at a wavelength of 520 nm. The non-collimated laser beam with a size of about 6 × 2 mm^2 was focused into a uniform 6 mm wide light sheet using a cylindrical lens (*f* = 200 mm). The resulting waist thickness was on the order of 200 µm before entering the wind tunnel glass panel from below (see Figure 1, left). Two imaging configurations were chosen. A 180 mm lens (*Zeiss Sonnar* T2.8/180) with extension tube imaged the complete boundary layer thickness (*m* = 0.47). Increased spatial resolution with *m* = 1.1 magnification factor was provided by a 400 mm lens (*Zeiss Makro Planar* T2.0/100 with two *Zeiss Mutar II* 2x teleconverters). The images were recorded with a CMOS high-speed camera (*PCO Dimax-S4*, 36GB) with a reduced field of view of 200 pixels width that allows the capture of up to 63,464 double-images at an image height of 1008 pixels. In order to keep the particle displacements at moderate levels around 30 pixels the laser pulse separation was set to Δt = 80 µs at U_∞ = 10 m/s and *m* = 0.47, and reduced proportionally at higher magnification (c.f. Table 1).

The acquired data was processed using a conventional 2-C PIV processing package featuring a coarse-to-fine resolution pyramid with intermediate image deformation (*PIVview2C*, *PIVTEC GmbH*, Germany). To obtain reliable mean velocity data and statistics within close proximity to the wall a high aspect ratio image sampling window of 64 pixels width and 12 pixels height was chosen. This corresponds to 1.5 × 0.28 mm^2 at *m* = 0.47 and 0.64 × 0.12 mm^2 at *m* = 1.1. For the latter the sample has an effective size of $17.5x^+ \times 3.28y^+$ at U_∞ = 10 m/s. The sample overlap was set at 75%.

Table 1: 2C-PIV image acquisition parameters

Magnification	*m*	-	***m* = 0.47**	***m* = 1.10**
Image size	(W x H)	pixels	200 x 2016	200 x 1008
Number of samples	*N*	-	31,738	63,464
Sample frequency	f_{acq}	Hz	2,000	4000
Laser pulse separation at 10 m/s	Δt	µs	80	40
Sequence length	*T*	s	15.87	15.87
BL turnover times at 10 m/s	$T\,U_\infty / \delta$	-	4,480	4,480
Eddy turnover times	$T\,u_\tau / \delta$	-	187.4	187.4

In a second step a STB measurement was performed at the same streamwise wall position and wind tunnel operating conditions. Illumination was realized using a *Quantronix DarwinDuo* Nd:YLF high-repetition laser with ~4 mJ energy per pulse at a repetition frequency of 15.873 kHz (two cavities operating at 7.937 kHz). The circular laser beam was shaped into an oval light profile, collimated, cut by a knife-edge and back-reflected onto itself by a mirror placed at the opposite side wall in order to increase the particle light scattering intensity for all in-line viewing directions. The rectangular shaped laser beam crossed the test section in spanwise directions and was aligned with the wall as close as possible. With a reduced resolution of 528 x 420 pixel four *PCO Dimax-S4* arranged in an in-line camera set-up below the wind tunnel enables a

high frame rate imaging of the illuminated particles in the measurement volume. Volumetric camera calibration was performed by using a 2D-glass target imaged at two planes with 2 mm separation. Volume-self-calibration [31] reduces the initial calibration error down to 0.1 px and parametrization of the OTF [32] was performed in order to account for present astigmatism effects at particle images during STB evaluation. At a magnification factor of ~1:3 and 11 µm per pixel, one pixel corresponds to 30 µm leading to a size of the measurement volume in *x*-*z*-directions of ~16 x 16 mm^2 (see illuminated area in Figure 1 (right)). This field is large enough to resolve a few near-wall low-speed streaks with an estimated average spanwise distance of $z^+ = 100$. In wall normal direction (y) the homogenous part of the light volume was about 1.2 mm thick which corresponds to an upper border of the 3D domain at $y^+ = 32$. Within the volume velocities up to $u = 7$ m/s corresponded to particle image shifts of ~13 pixels at the given 15.873 kHz frame rate, which is well suited for the STB tracking algorithm as most of the particles stay inside the volume for more than 40 time steps. For STB evaluation a predictor was used, which was gained from a STB pre-evaluation in form of a velocity profile. Additionally, its local rms-values for all three components have been used in order to regularize the particle search and shake radius (0.3 px + 5 times the local rms-component). Important values of the STB set-up are given in Table 2.

The aim of the present investigation is to acquire the full 3D velocity vector field of irregularly distributed particle tracks including the viscous sub-layer and the buffer layer with the region of the maximum stream-wise fluctuations $<u'u'>^+$ at $y^+ \sim 13$. At particle image densities between approximately 0.015 and 0.035 ppp (particles per pixel) up to 5,700 particles could be identified and tracked by STB for each time step. Of these particles approximately 700 particles are contained in the viscous sub-layer below $y^+ = 5$ and can be used to estimate the time-resolved skin friction velocity vector field in the measurement area of 16 x 16 mm or 430 x 430 viscous units for both stream- and spanwise components u_τ and w_τ using the dynamic viscosity µ and the near-wall velocity gradients *du/dy* and *dw/dy* respectively.

From ~ 230,000 time steps corresponding to 4,093 boundary layer turn over times U/δ or ~140 eddy turn over times u_τ/δ reasonable statistics of the near-wall mean velocity profile, together with all Reynolds stresses respectively skin friction velocity components, were then calculated from the volumetric Lagrangian track results from STB evaluation. The exact wall position was extracted from spatially highly resolved mean velocity profiles using bin averaging of the STB tracks in bin sizes of 1/13th l^+ at four sub-volume locations and extrapolating the linear profile between $2 < y^+ < 4.5$ to zero *u*-velocity. After estimation of the wall position span- and streamwise symmetry in a statistical sense for the relatively small volume can be assumed, so that wall normal 1D-profiles with a very high spatial resolution and high number of independent velocity data per bin can be extracted. The averaging process corresponds to 14.49 sec integration time at 15.873 kHz frame rate using ~$8 \cdot 10^8$ data points.

Table 2: STB image acquisition parameters

Magnification	m	-	$\boldsymbol{m = 0.36}$
Image size (each of four cameras)	(W x H)	pixels	528 x 420
Number of samples	N	-	230,000
Sample frequency	f_{acq}	Hz	15,873
Laser pulse separation ($1/f_{acq}$)	Δt	µs	63
Sequence length	T	s	14.49
BL turnover times at 10 m/s	$T\,U_\infty / \delta$	-	4,093
Eddy turnover times	$T\,u_\tau / \delta$	-	172.3

Figure 1: *Left:* Imaging setup for boundary layer profile measurements by high-repetiton-2C-PIV in the 1m-Wind Tunnel of DLR Göttingen. *Middle:* Collimated laser light volume with passe-partouts parallel to the wall *Right*: In-line camera high-repetition STB set-up with four *PCO Dimax-S4* cameras viewing through a glass insert of the wall.

BOUNDARY LAYER CHARACTERIZATION

As demonstrated in [30] the velocity profile and, in particular, the accompanying higher order statistics of a turbulent boundary can be obtained using long continuous PIV records of length $O(10^4\text{-}10^5)$. With a few modifications the methodology is extended for the present wind tunnel application. Two challenges had to be addressed: the distance to the measurement location is increased to about 550 mm while at the same time the free stream velocity was increased from 5 m/s up to 10 m/s. The latter results in a reduction of the viscous length scale which requires an increase in spatial resolution on the detector side. At the same time the higher velocity and higher magnification entails a proportionate reduction of the laser pulse separation.

Estimates of the mean and unsteady wall shear rate $\gamma = du/dy|_0$ were obtained using a single-line cross-correlation approach as described in [30] (i.e. the sampling window only has a wall-normal size of one pixel). The characteristic parameters for the boundary layer are summarized in Table 3. The measured data is normalized with inner variables using the traditional viscous scaling for velocity u_i^+ (= u_i/u_τ) and length l_i^+ (= $l_i\, u_\tau/\nu$). In this sense the mean velocity profiles for u for both Reynolds numbers are shown in Figure 2 (left). The corresponding Reynolds stress variances $\langle u'u'\rangle^+$, $\langle v'v'\rangle^+$ and covariances $\langle u'v'\rangle^+$, are provided in Figure 2 (right). Both pairs of plots also contain reference data from a DNS of a ZPG TBL provided by Schlatter et al. [18]. For the most part, the agreement between experiment and simulation is very good (the lines nearly coincide). Several discrepancies can be observed nonetheless: in the experiment the wake region above $y^+ > 200$ is less pronounced while the peaks of the streamwise variances are shifted outward by 1-2y^+. In the near wall region ($y^+ < 10$) the finite sized sample window results in significant departure from the predicted nearly linear velocity behavior, especially at the lower magnification.

Plots of the third and fourth moments of the streamwise velocity u are presented in Figure 3. While overall agreement between experiment and DNS is good, discrepancies do arise due to finite sample size and quite possibly the limited number of samples.

Table 3: Characteristic quantities of studied ZPG-TBL obtained with high-resolution 2C-PIV

	Symbol	**Unit**	$\boldsymbol{Re_\theta = 2770}$
Tunnel free stream velocity	U_∞	m s^{-1}	10.0
Magnification factor (low / high res.)	m	-	0.47 / 1.1
Magnification on sensor (low / high res.)	m	µm pixel^{-1}	23.6 / 10.0
Measured free stream velocity	U_∞	m s^{-1}	10.09
Boundary layer thickness at 0.99 U_∞	δ_{99}	mm	35.4
Displacement thickness	δ^*	mm	5.75
Momentum thickness	θ	mm	4.16
Shape factor	H	-	1.384
Friction coefficient	C_f	-	0.00317
Wall shear rate, estimated	$du/dy\|_0$	s^{-1}	11350
Friction velocity	u_τ	m s^{-1}	0.418
Viscous unit	ν/u_τ	µm	36.58
Wall unit on sensor (high / low res.)	ν/u_τ	pixel	1.56 / 3.68
Reynolds number	Re_δ	-	23515
Momentum Reynolds number	Re_θ	-	2768
Friction Reynolds number	Re_τ	-	961

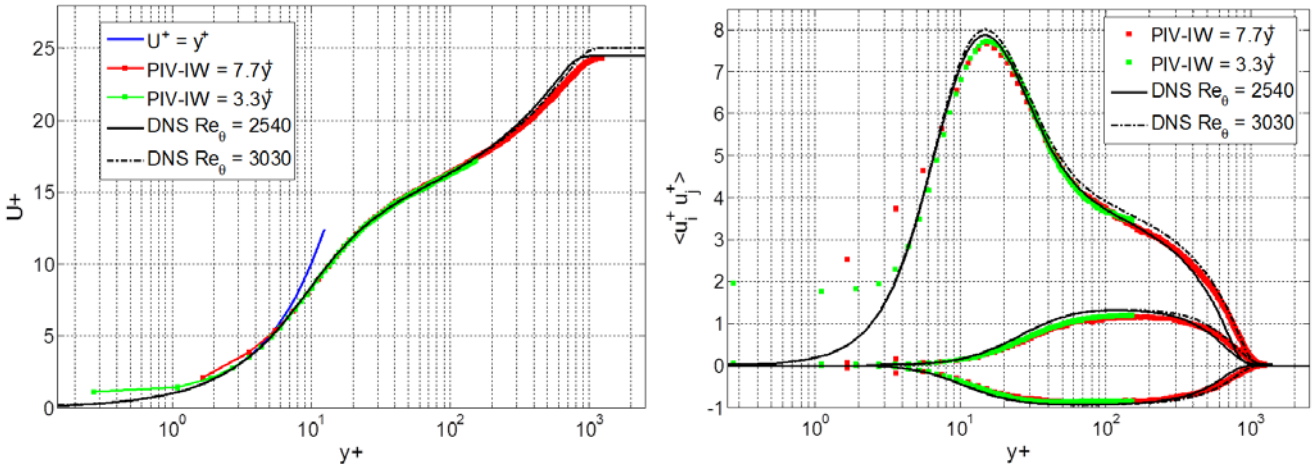

Figure 2: Mean velocity profiles at U_∞ = 10 m/s; (left) and inner-normalized profiles of the velocity variances from the high-resolution 2C-PIV measurements; top curve set represents $<u'u'>^+$, middle curve set $<v'v'>^+$, bottom curve set $<u'v'>^+$. Black lines DNS data from Schlatter et al. [18]

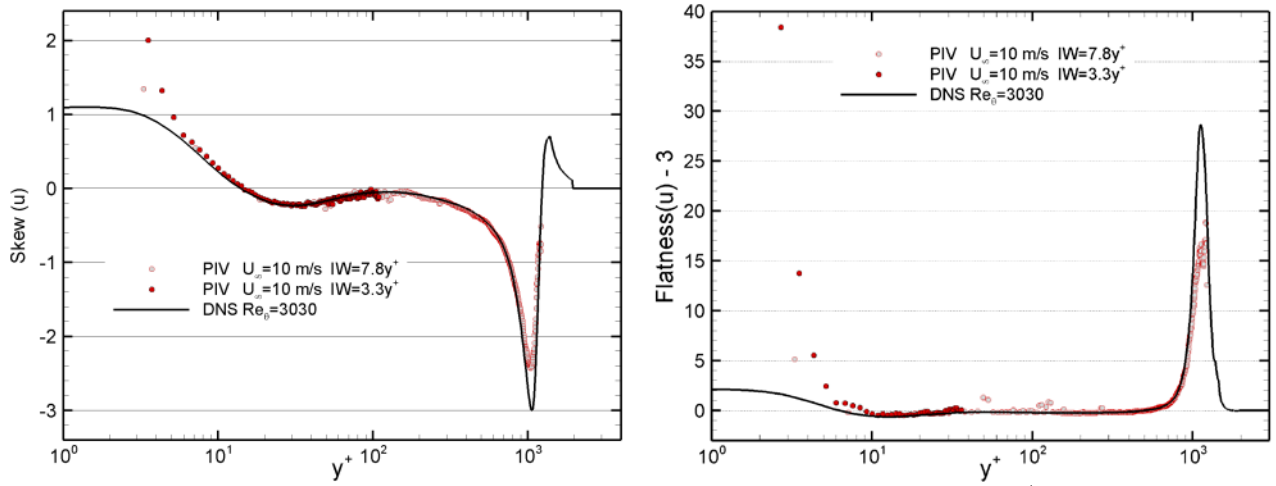

Figure 3: Profiles of the streamwise velocity skewness (left) and flatness (right) plotted versus y^+ (Flatness of 3 corresponds to a Gaussian distribution) ; black lines DNS data from Schlatter et al. [18]

NEAR-WALL STB RESULTS

An example of measured instantaneous velocity vectors distributed irregularly within a wall-parallel volume of approximately 16 x 1.4 x 16 mm³ according to 430 x 36 x 430 viscous units $(l^+)^3$ in *x*-, *y*- and *z*-directions evaluated by STB is shown in Figure 4. The velocity vectors are color coded by the *u*-velocity component and based on the application of an optimal temporal Wiener filter along 19 subsequent time steps of the reconstructed 3D Lagrangian particle tracks. The kernel size of the temporal Wiener filter is in the order of the Kolmogorov time scales η. The relatively dense Lagrangian tracks are built along two 7.27 s long time series of 115,000 particle images per set. Within the three projections of ~5,700 instantaneous velocity vectors onto the respective side planes of the measurement volume displayed in Figure 4 the typical features of a turbulent boundary layer flow in close proximity to the wall can be identified. High and low-speed flow regions elongated in flow directions are visible in the *x*-*z*-projection, while a spanwise meandering of these streaky regions with respective spanwise velocity components are as well detectable in the *y*-*z*-projection. Here in the top area of the projected volume (Figure 4, right) a spatially organized sweep (Q4-) event is combined with relatively large spanwise velocities, which, following the temporal development in the time-resolved series, can be generally addressed to be precursors for strong ejection (Q2-) events. Underneath these events the very low-velocity distribution (< 1 m/s) in the area

within and slightly above the viscous sublayer (y^+ < 183 µm) is more extended in wall-normal direction within low-speed streak regions and "compressed" to a thinner layer in high-speed streak or sweep regions. The *x*-*y*-projection shows the typical TBL *u*-velocity profile and respective strong instantaneous (wall-) shear gradients $du/dy|_{>0}$. As the particle position estimation using STB in experimental investigations is ideally in the order of less than 0.1 pixels which on top is filtered temporally (in the order of η) a very accurate velocity estimation close to the wall can be reached. This is particularly the case for the low-velocity particles near the wall that stay in the measurement volume for up to several hundred time-steps and the respective tracks are temporally highly oversampled with respect to the maximum acceleration values or smallest Kolmogorov time scales η, which are typically in the order of a viscous unit for TBL close to the wall [26].

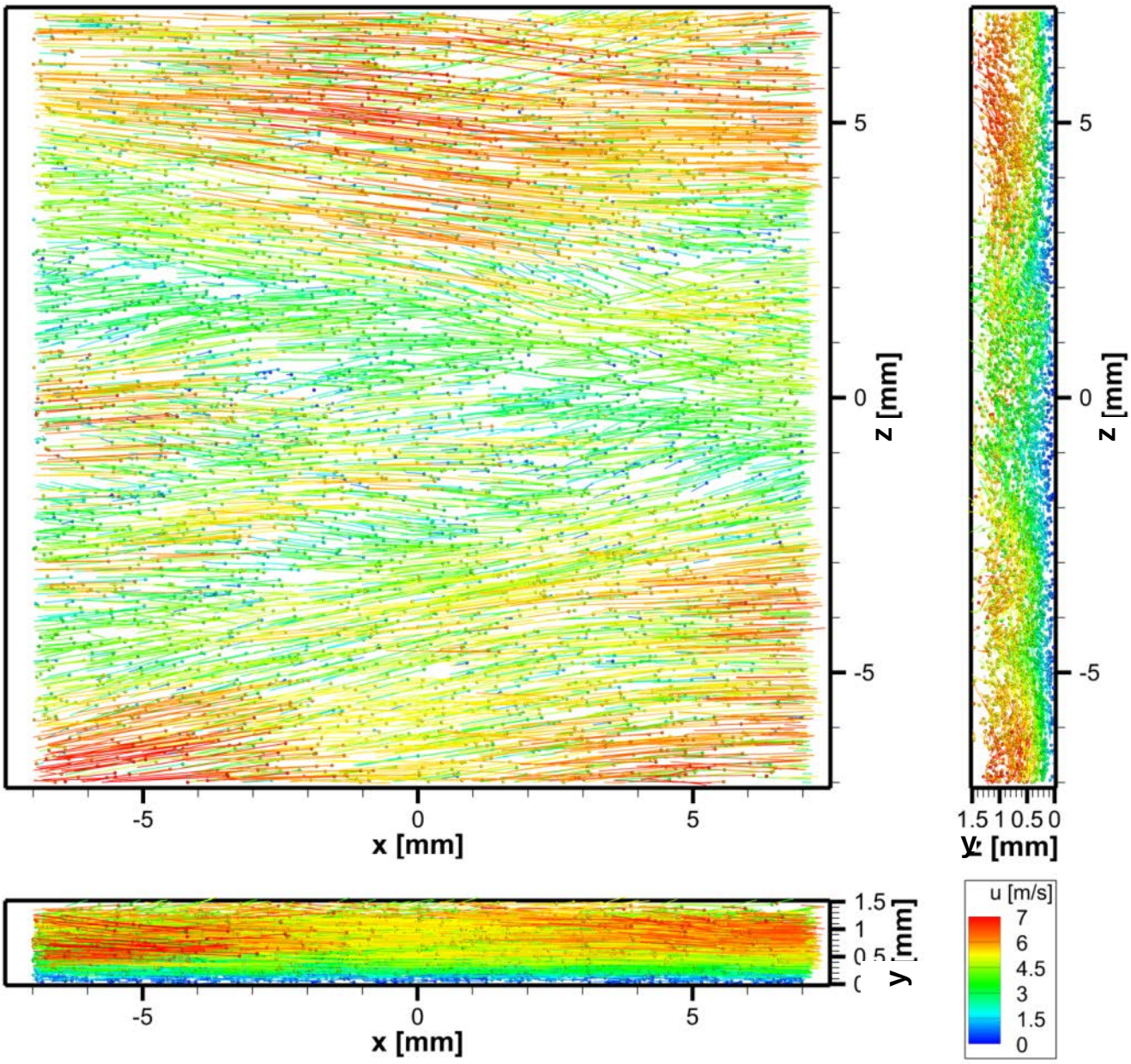

Figure 4: Instantaneous velocity vector distribution from optimal Wiener filtered Lagrangian tracks with ~5,700 particles in a volume of the TBL close to the wall projected onto x-z- (top-left), y-z- (right) and x-y- planes (bottom) of the STB measurement volume (u-comp of velocity color coded, y = 1.4 mm corresponds to ~36 viscous or wall units)

The total amount of data points ~8 x10^8 are available from the two STB runs for calculating a wall-normal 1D-profile in a bin averaging approach (projecting span- and streamwise extensions) including all components of the velocity vector and Reynolds stress tensor in bin sizes of 0.1 pixel resp. 1/13th l^+. Depending on the intensity profile of the volumetric illumination and boundary effects of the STB evaluation approach the number of detected particle tracks varies along the respective wall normal row of bins. In Figure 5 (left) the number of samples collected in each bin along y^+ is displayed. In the region between y^+ = 1.5 and y^+ = 32 for both runs more than 1 x 10^6 samples are available, which are mostly statistically independent although there is a high time-resolution of the measurement. Due to the span- and streamwise projection onto a one-dimensional wall normal line along 14.49 s integration time these bin entries are statistically fully converged. In the area below y^+ = 1.5 and above y^+ = 32 boundary effects of the STB evaluation occurs mainly due to a reduction of the illumination intensity very close to the wall and some tracking issues due to out-of-focus particles above y^+ = 32. Nevertheless, here more than 1 x 10^5 entries could be collected.

A linear representation of the mean *u*-velocity profile along y^+ is given in Figure 5 (right) together with the scatter plot of the respective instantaneous *u*-velocity samples (blue scatter) of a small sub-set of the available data. It is clearly visible that almost all instantaneous velocity events fall in between the two black lines above and below the blue area which represent the boundaries of the STB track building approach.

The STB result of the converged U^+ velocity mean profile is given by the red squares along y^+ in Figure 6 in logarithmic (top left) and linear (top right) representation. The comparison with the black line given by DNS at Re_θ = 2540 [18] and with the green squares from measurement results of the high-resolution 2C PIV method show the advantages of the fully 3D particle tracking approach. The measured mean profile by STB follows exactly the DNS line down to ~ y^+ = 1.4 with only minor deviations which can be accredited to the slightly different Reynolds number and experimental boundary conditions (e.g. wall roughness). A direct comparison with the 2C PIV measurement confirms basically the low-pass filtering effect of the correlation based (even single-pixel line) approaches in comparison to the well resolved STB approach. The important statistic values for the TBL near-wall region characteristics determined by the STB bin averaging results are given in Table 3. Due to slight changes in temperature and pressure at the STB- compared to the 2C-PIV measurement the flow parameters changed slightly resulting in a Reynolds number of Re_τ = 929. This Reynolds number is based on the friction velocity of u_τ = 0.4042 m/s estimated by a linear fitting along the STB bin averaged mean *u*-velocity profile between y^+ = 2 and y^+ = 4.5, which can be considered to be statistically converged. The 2C-PIV friction velocity estimation of u_τ = 0.418 m/s has been obtained by the single-pixel line evaluation technique method and relies on the respective accuracy of the 2C-PIV profile measurement in the near wall region of the higher magnification factor displayed in Figure 2 (left). Accordingly, all the inner-scaled parameters differ slightly between 2C-PIV and STB results.

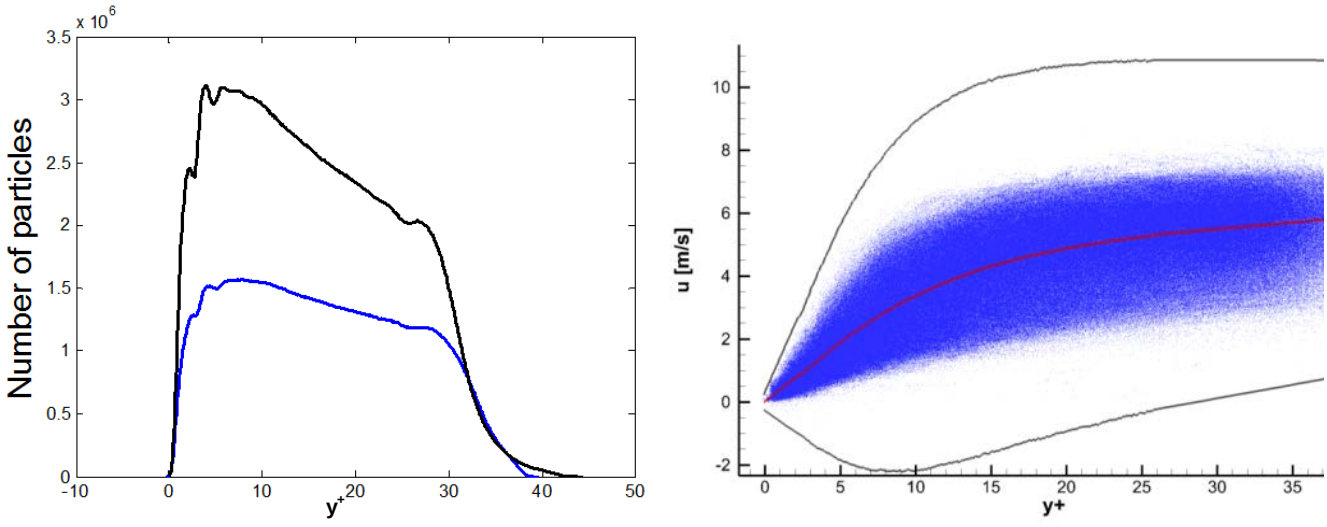

Figure 5: Number of particles with velocity vector information per bin size of 0.1 pixel resp. 1/13th l^+ averaged over two runs (blue and black) with different particle image densities (ppp) along y^+ (left). Mean *u*-velocity profile (red) and scatter plot of instantaneous *u*-velocity entries (blue dots) of a sub-set of the available STB velocity data. Black lines indicate upper and lower track building boundaries of the STB evaluation scheme (right)

Table 3: Characteristic quantities of studied ZPG-TBL obtained with STB

	Symbol	**Unit**	$\boldsymbol{Re_\theta = 2770}$
Tunnel free stream velocity	U_∞	m s^{-1}	10.0
Magnification factor	m	-	0.36
Magnification on sensor (low / high res.)	m	µm $pixel^{-1}$	30
Measured free stream velocity	U_∞	m s^{-1}	10.00
Friction coefficient	C_f	-	0.003266
Wall shear rate, estimated	$du/dy\|_0$	s^{-1}	10480
Mean wall shear stress	$\mu\ du/dy\|_0$	kg $m^{-1}s^{-2}$	0.1933
U-rms wall shear stress (u-rms)/(mean)		-	0.396
Friction velocity	u_τ	m s^{-1}	0.4042
Viscous unit	ν/u_τ	µm	38.39
Wall unit on sensor	ν/u_τ	pixel	1.3
Friction Reynolds number	Re_τ	-	929

Nevertheless, maybe due to the strong reduction of the illumination intensity very close to the wall which is an intrinsic problem of a collimated tangential illumination mainly due to refraction along the surface a slight bias towards higher velocities can be detected in the mean velocity statistic below $y^+ = 1.5$ in Figure 6 (top-left). The expected spatial resolution of the STB bin averaging approach should be in the range of the positional uncertainty of the 3D particle reconstruction which is around 0.1 px for experimental data [15] or the used bin size. Therefore there is the suspicion that a systematic issue which correlates with the low illumination intensity is crucial: the signal-to-noise ratio of the particles very close to the wall is pretty low, which increases the trend of a pixel-locked representation of the particle position. This results in a 3D pattern of superimposed lines-of-sight of each camera pixel, which at their 3D knot distribution biased particle positions agglomerate and thus as well causes velocity biases (here towards higher velocities). Most probably this pattern biases the results in the near wall regions a bit more due to the fact that at low velocities the temporal filtering effect of such errors is further reduced. Such issues have to be addressed in future STB measurements of near wall TBL flow investigations by proper illumination strategies as the reachable spatial resolution resp. 3D particle positional- and related velocity estimation accuracy for well illuminated particles can be much higher [13].

The components of the Reynolds stresses show a very good agreement between the STB results of the $<u'u'>^+$ and the related DNS data down to sub- viscous units in the near wall region. Also the $<v'v'>^+$ profile of STB closely follows the DNS line, which at the same time lead to a nearly perfect alignment of STB and DNS data for the covariance $<u'v'>^+$ profile, with only a slight drift to lower measures for larger y^+ values. Note that the upper part of that profile is also well resolved by the 2C PIV approach and both experimental methods show the same trend, so that those small differences might be physical and relate to the wind tunnel conditions. Furthermore, the $<w'w'>^+$ profile from STB is also very close to the DNS data, but shows slightly lower values of the spanwise variances. Again the slight deviation could be accredited to the wind tunnel conditions.

In general so far no measurement technique is known to the authors which enables a more accurate and higher resolution profile of all components of the (mean) velocity vector and the full Reynolds stress tensor for such small viscous unit sizes without intrusiveness and band pass filtering effects within short measurement times. The use of PTV measurement tools for obtaining accurate profile measurements close to walls is motivated by the assessment done by Kähler et al. [33]. But especially the additional possibility to measure the full frequency range of all 3D velocity vectors and both components of the wall-shear stress fluctuation vectors at many points simultaneously in a relatively large volume resp. area at the wall with a high spatial resolution and without band pass filtering effects is a unique feature of the STB method. The analysis of the temporal resolution of the present data-set has not been explored yet. It would enable bin averaged 3D two-point space-time correlations for the determination of Taylor micro- and macro scales at various wall distances and e.g. the convection velocities, frequency analyses and the calculation of spectra of different velocity components or the wall-shear stress components. Unfortunately the full potential of the spatial accuracy of the STB technique at the very near wall region could not be reached in the present study for two reasons. Following the aforementioned problem of the near wall particle illumination and resulting bias issues below $y^+ = 1.5$ the accuracy of the STB variance measurement is also slightly lower resulting, for instance, in small positive values for $<u'u'>^+$ very close to the wall. Secondly, regarding the lower temporal filtering effect close to the wall a locally adapted optimal temporal Wiener fit length very close to the wall would be advantageous. Both, the illumination issue and temporal filtering adaptation can be easily solved by performing STB experiments in (TBL) water flows, which would allow the use of larger particle sizes and a full temporal resolution at lower frame rates and laser repetition frequencies at much higher Reynolds numbers.

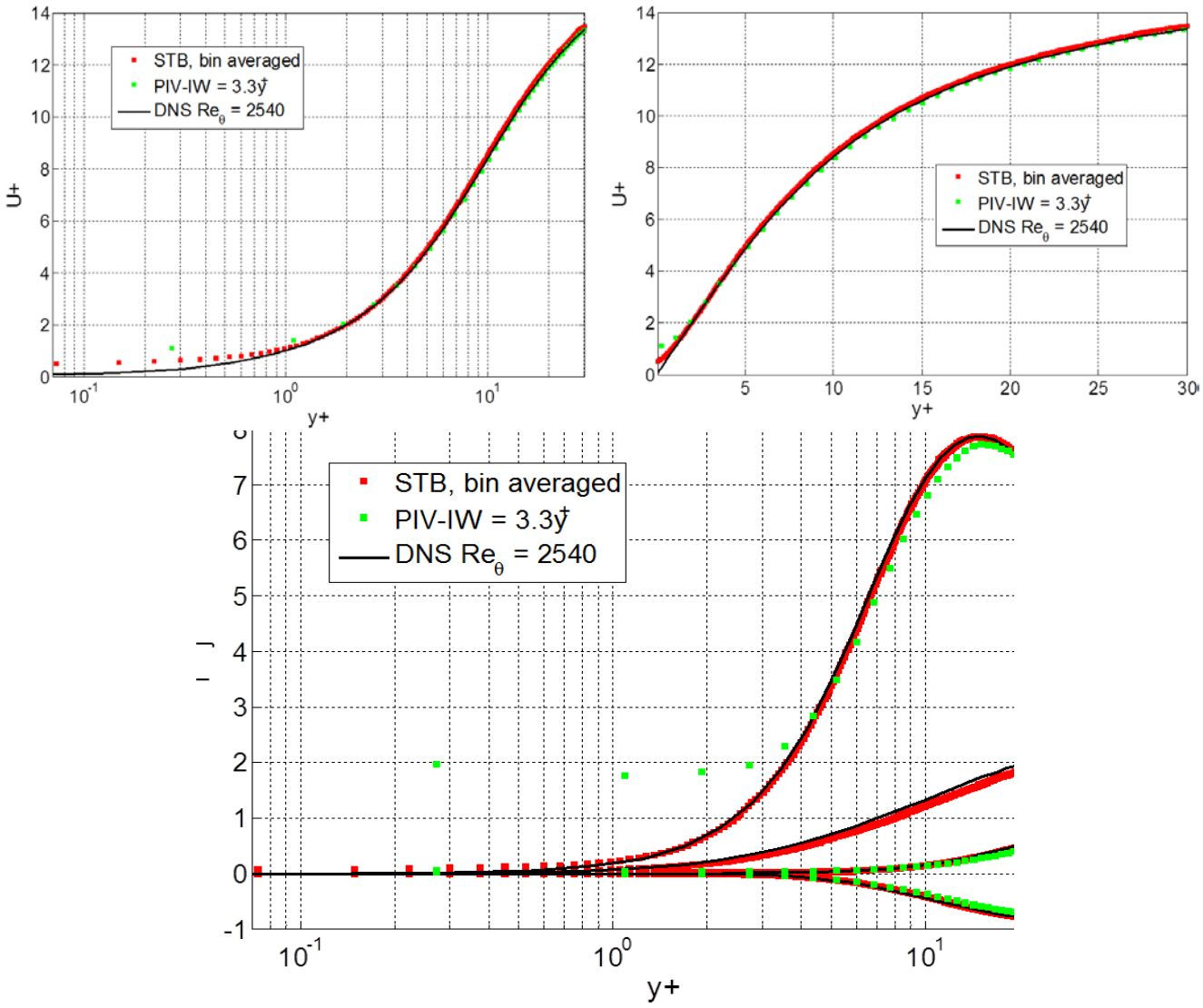

Figure 6: Inner-normalized mean velocity profiles U^+ against wall distance y^+ scaled logarithmically (left) and linear (right) and respective profiles of the velocity variances (bottom) at U_∞ = 10 m/s. At the velocity variances or Reynolds stresses (bottom) the top curve represents $<u'u'>^+$, middle curves set $<w'w'>^+$ (upper) and $<v'v'>^+$ (lower), bottom curve set $<u'v'>^+$. Red squares are STB results with 0.1 pixels or 1/13th l^+ spatial resolution, green squares are from 2C-PIV (see Fig 2) and black lines are from DNS data at Re_θ = 2540 [18].

The rms-value of the *u*-component of the wall-shear stress has been estimated to $\tau^+_{w,\,rms}$ = 0.396 from the STB evaluated instantaneous velocity gradients $du/dy|_0$ of all particles between y^+ = 2 and y^+ = 4.5. This value fits quite well to 0.4 given by [35], while the formula given in [18] would result in $\tau^+_{w,\,rms}$ = 0.421 for the present Re_τ. Looking on the corresponding probability density function of the fluctuation values of τ^+_w(u) in a linear representation estimated from the bin averaged STB results in Figure 7 (left) one can see a very good agreement for a respective DNS result given in Hu et al. [36] in Figure 7 (right). A possible explanation for the slightly lower rms-value compared to DNS data from [18][20][34][37] is visible in Figure 8. Here the same probability density function of the instantaneous τ^+_w(u) without subtraction of the mean value is displayed in a logarithmic representation. In comparison to DNS STB shows lower maximal values for the rare extreme events on the negative and positive ends of the respective distribution (Figure 8 (left)). Although a few negative values are present, which implies measured reverse flow in the respective STB interrogation area, the extreme values very close to the wall have not been considered by STB in the present investigation due to the mentioned illumination issues and chosen physical boundaries for gaining a reliable track building process (see black lines in Figure 5 (right)).

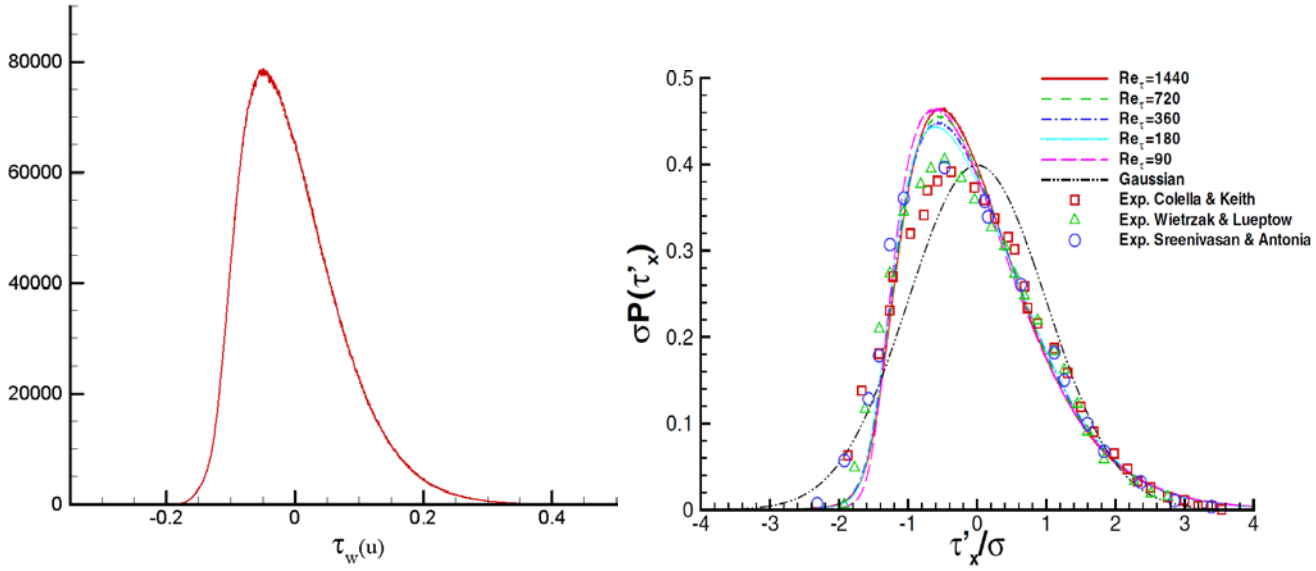

Figure 7: Probability density function (arbitrary units) of the *u*-component of the wall-shear stress fluctuations in a linear representation from STB (left) and DNS values at similar Reynolds numbers normalized by σ from Hu et al , Figure 10 [36] estimated from turbulent channel flow (right)

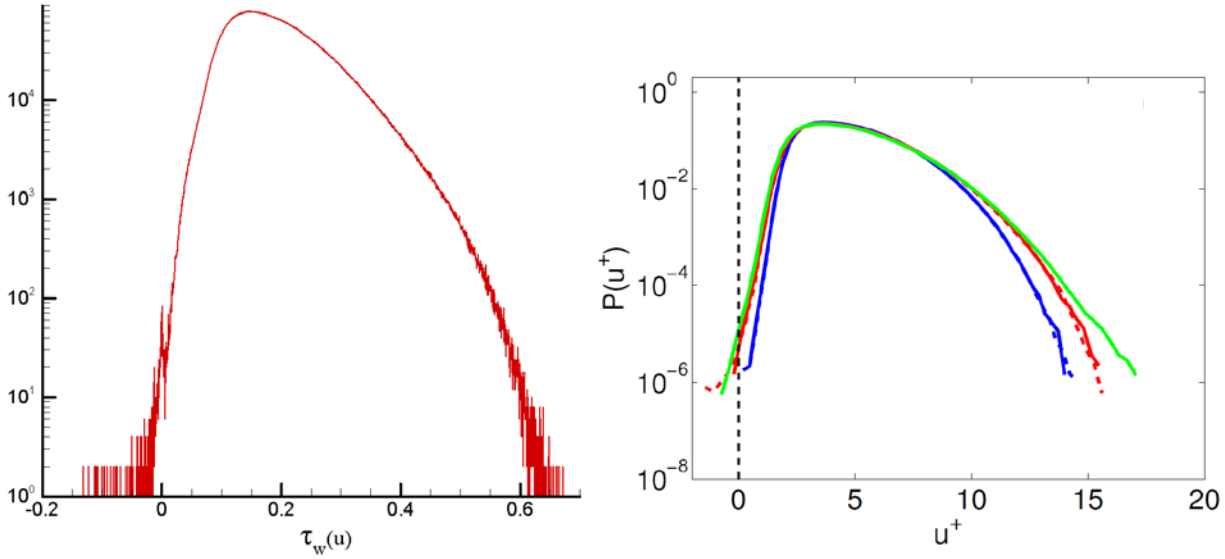

Figure 8: PDF of the wall-shear stress in a logarithmic representation showing rare negative values (reverse flow events) (left) and PDF of u^+-velocity fluctuations for three different Reynolds number (green line at Re_τ= 1000) from DNS data from Lenaers et al., Figure 4 [20]

It can definitely be stated that excluding the near wall position below $y^+ = 2$ for the estimation of the instantaneous wall-shear stresses decreases the number of rare and extreme wall-shear stress events, which can be confirmed by the similarity of the PDF of the present wall-shear stress estimation by STB in Figure 8 (left) and the shape of a PDF of the *u*-velocity fluctuations from a respective turbulent channel flow DNS [19] at a constant wall distance of $y^+ = 5$ displayed in Figure 8 (right). The number of negative (extreme) wall-shear stress events decreases with the wall distance and increases with the Reynolds number. A new computation of the present STB data including values closer to the wall would deliver a wider distribution of the wall-shear stress and more extreme events, but the main problem is again to enable a very accurate estimation of the velocity gradient even below $y^+ = 1$. The big challenge for measurements techniques in close proximity to surfaces is that every little uncertainty of the measured instantaneous velocity is significantly increased by calculating the

gradient $du/dy|_0$ when approaching the wall, because the value in the denominator approaches zero. In principle STB could provide the required high accuracies because a very good oversampling in time for those particles close to wall is given. For reaching the goal of calculating exact wall-shear stress values below $y^+ = 1$, beside the illumination issue, STB needs to be adapted with a local optimal temporal filtering approach close to the wall as already mentioned above.

CONCLUSIONS AND OUTLOOK

Two advanced particle based measurement methods, high-resolution high-speed 2C-PIV and STB, have been applied to a zero pressure gradient turbulent boundary layer (TBL) flow at $Re_\tau = 960$ and $Re_\tau = 929$ respectively. Both methods work very efficiently in delivering statistically converged and relevant data of mean and fluctuation velocity components for the overall characterization of the TBL within short measurement and evaluation times. The 2C-PIV method has the additional advantage of being simple and compact on the experimental side. While STB needs a high-power high-speed laser and four high-repetition frame rate cameras in a tomographic set-up, the evaluation time of only ~6 sec per time step on a simple multi-core computer for the STB track building is also very efficient for a 4D technique, mainly because of the limited amount of particles (3,000 to 6,000) to be reconstructed. Significant advantages of the STB 4D-PTV technique have been demonstrated in terms of accuracy, spatial and temporal resolution. STB delivers a well converged 3D data set of relatively dense Lagrangian tracks and related time resolved velocity vector volumes. The full Reynolds stress tensor has been determined based on a bin averaging process leading to a spatial resolution down to a fraction of a viscous unit (wall unit). The profiles of the mean velocity, components of the Reynolds stress tensor and the PDF of the instantaneous wall-shear stress distribution show very good agreement with DNS data at similar Reynolds numbers, in particular for the highly resolved STB data. Some adaptive steps on the hardware and evaluation side of STB could be identified to gain even better results for very near-wall velocity and instantaneous wall-shear stress measurements. With this first application of STB to a TBL flow in air the technique is proven capable to deliver valuable time-resolved 3D data in a non-intrusive manner. Further possibilities in extracting and analyzing Lagrangian and Eulerian properties of the near-wall dynamics are still open. In the future the application of the STB technique to higher Reynolds number TBL flows in water (beyond the possibilities of present DNS and comparable to those from earlier investigations [38]) shall further demonstrate the capabilities of STB in delivering accurate data for temporally and spatially highly resolved turbulence characterizations.

REFERENCES

[1] Alfredsson PH, Örlü R, Schlatter P "The viscous sublayer revisted-exploiting self-similarity to determine the wall position and friction velocity", Exp Fluids (2011) 51: 271-280

[2] Compton DA, Eaton JK "A high-resolution laser doppler anemometer for three-dimensional turbulent boundary layers", Exp Fluids (1996) 22: 111–117

[3] Fischer M, Jovanovic J, Durst F "Reynolds number effects in the near-wall region of turbulent channel flows", Phys Fluids (2001) 13, 6

[4] Tanner LH, Blows LG "A study of the motion of oil films on surfaces in air flow, with application to the measurement of skin friction", J Physics E, Scientific Instruments 9 (1976)

[5] Monson DJ "A nonintrusive laser interferometer method for measurement of skin friction", Exp Fluids (1983) 1: 15–22

[6] Raffel M, Willert C, Wereley S, Kompenhans J "Particle image velocimetry: a practical guide", Exp Fluid Mech (2007), Springer, Berlin

[7] Elsinga GE, Scarano F, Wieneke B and van Oudheusden BW "Tomographic particle image velocimetry", Exp Fluids (2010) 41: 933-947

[8] Schröder A, Geisler R, Staack K, Elsinga G, Scarano F, Wieneke B, Henning A, Poelma C, Westerweel J "*Eulerian and Lagrangian views of a turbulent boundary layer flow using time-resolved tomographic PIV*", Exp Fluids (2011) 50: 1071–1091.

[9] Adrian RJ "Dynamic ranges of velocity and spatial resolution of particle image velocimetry", Meas Sci Technol (1997) 8(12):1393

[10] Kähler CJ, Scholz U, Ortmanns J "Wall-shear-stress and near-wall turbulence measurements up to single pixel resolution by means of long-distance micro-PIV," Exp Fluids (2006) 41: 327–341

[11] Sheng J, Malkiel E, Katz J "Using digital holographic microscopy for simultaneous measurements of 3D near wall velocity and wall shear stress in a turbulent boundary layer", Exp Fluids (2008) 45:1023–1035

[12] Schanz D, Schröder A, Gesemann S, Michaelis D and Wieneke B "Shake-the-Box: a highly efficient and accurate Tomographic Particle Tracking Velocimetry (TOMO-PTV) method using prediction of particle position", 10th Symp PIV (2013) Delft, The Netherlands

[13] Schanz D, Schröder A and Gesemann S "Shake-the-Box - a 4D PTV algorithm: accurate and ghostless reconstruction of Lagrangian tracks in densely seeded flows", 17th Symp Laser Tech (2014) Lisbon, Portugal

[14] Wieneke B "Iterative reconstruction of volumetric particle distribution", Meas Sci Technol (2013) 24, 024008

[15] Schröder A, Schanz D, Michaelis D, Cierpka C, Scharnowski S and Kähler CJ "Advances of PIV and 4D-PTV "Shake-The-Box" for Turbulent Flow Analysis – the Flow over Periodic Hills" Flow, Turbulence and Combustion (2015), 17p, Published online, May 24, DOI 10.1007/s10494-015-9616-2

[16] Bruecker C, “Evidence of rare backflow and skin-friction critical points in near-wall turbulence using micropillar imaging” Phys Fluids (2015), 27, 031705

[17] Örlü R, Fransson JHM and Alfredsson PH “On near wall measurements of wall bounded flows—the necessity of an accurate determination of the wall position”, Prog Aero Sci (2010) 46:353–387

[18] Schlatter P and Örlü R “Assessment of direct numerical simulation data of turbulent boundary layers”, J Fluid Mech (2010) 659: 116–126.

[19] Mathis R, Marusic I, Chernyshenko SI, Hutchins N “Estimating wall-shear-stress fluctuations given an outer region input”, J Fluid Mech (2013) 715: 163-180

[20] Lenaers P, Li Q, Brethouwer G, Schlatter P and Örlü R „Negative streamwise velocities and other rare events”, J Phys: Conference Series (ETC13) (2011) 318, 022013

[21] Cardesa J, Monty J, Soria J, Chong M. “Skin-friction critical points in wall-bounded flows,” J Phys. (2014): Conf. Ser. 506, 012009

[22] Eckelmann H “The structure of the viscous sublayer and the adjacent wall region in a turbulent channel flow”, J Fluid Mech (1974) 65:439–459

[23] Große S and Schröder W “Wall-shear stress patterns of coherent structures in turbulent duct flow”, J Fluid Mech (2009) 633

[24] Amili O and Soria J “Wall shear stress distribution in a turbulent channel flow”, 15th International Symposium on Applications of Laser Techniques to Fluid Mechanics, Lisbon, Portugal, 05–08 July, (2010).

[25] Cierpka C, Scharnowski S, Kähler CJ “Parallax correction for precise near-wall flow investigations using particle imaging”, Appl Opt (2013) 52: 2923-2931

[26] de Silva CM, Gnanamanickam EP, Atkinson C, Buchmann NA, Hutchins N, Soria J, Marusic I “ High-spatial range velocity measuremets in a high Reynolds number turbulent boundary layer”, Phys Fluids (2014) 26, 025117

[27] Novara M, Schanz D, Kähler CJ, Schröder A „Shake-The-Box for multi-pulse tomographic systems: towards high seeding density particle tracking in high speed flows, 11th Symp PIV (2015), St. Barbara, CA, USA

[28] Wu PP, Miles RB "High-energy pulse-burst laser system for megahertz-rate flow visualization", Opt Lett (2000) 25, 1639-1641

[29] Thurow B, Jiang N, Samimy M, Lempert W “Narrow-linewidth megahertz-rate pulse-burst laser for high-speed flow diagnostics”, Appl Optics (2004) 43, 26: 5064 - 5073

[30] Willert C H “High‑speed particle image velocimetry for the efficient measurement of turbulence statistics”, Exp Fluids (2015) 56: 17p

[31] Wieneke B “Volume self-calibration for 3D particle image velocimetry” Exp Fluids (2008), 45: 549-556

[32] Schanz D, Gesemann S, Schröder A, Wieneke B and Novara M “Non-uniform optical transfer function in particle imaging: calibration and application to tomographic reconstruction” Meas Sci Technol (2013) 24, 024009

[33] Kähler CJ, Scharnowski S and Cierpka C “On the uncertainty of digital PIV and PTV near walls”, Exp Fluids (2012) 52: 1641-1656

[34] Schlatter P, Örlü R, Li Q, Brethouwer G, Fransson JHM, Johansson AV, Alfredsson PH, Henningson DS “Turbulent boundary layers up to Re_θ = 2500 studied through simulation and experiment”, Phys Fluids (2009) 21(5), 051702

[35] Alfredsson PH, Johansson AV, Haritonidis J, Eckelmann H” The fluctuating wall-shear stress and the velocity field in the viscous sublayer, Phys Fluids 31 (1988) 31: 1016-1033.

[36] Hu ZW, Morfey CL, Sandham ND “Wall Pressure and Shear Stress Spectra from Direct Simulations of Channel Flow” AIAA Journal (2006) 44,7: 1541-1549

[37] Örlü R and Schlatter P “On the fluctuating wall shear stress in zero pressure-gradient turbulent boundary layer flows”, Phys Fluids (2011) 23, 21704

[38] Fernholz HH, Finley PJ “The Incompressible Zero-Pressure-Gradient Turbulent Boundary Layer: an Assessment of the Data”, Prog. Aerospace Science (1996) 32: 245-311